Available online at http://scik.org
Commun. Math. Biol. Neurosci. 2020, 2020:87
https://doi.org/10.28919/cmbn/4998
ISSN: 2052-2541

COMPARTMENTAL SEIRW COVID-19 OPTIMAL CONTROL MODEL

SACRIFICE NANA-KYERE[1,*], ERIC OKYERE[2], JOHNSON DE-GRAFT ANKAMAH[2]

[1]Department of Mathematics and Information Technology, Valley View University, Ghana

[2]Department of Mathematics and Statistics, University of Energy and Natural Resources, Ghana

Abstract. With no specific treatment identified, COVID-19 remains a major threat to the world, as the scientific community continues to look for a better understanding of the epidemiological cycle and dynamics of the virus. Mathematical modeling of the 2019 coronavirus disease may provide a better insight into the virus complex dynamics and lay preventive measures that can be employed to contain the disease from spreading. In this research article, a new compartmental SEIRW COVID-19 model is introduced and examined, to describe the dynamics of the disease. We have established both local and global stability analysis for the model equilibria computed from the mathematical model. Additionally, using personal protection, treatment, and spraying of disinfectant as time-dependent control functions, we have developed a SEIRW optimal control COVID-19 epidemic model. Applying the well-known Pontryagin's maximum principle and the constructed Hamiltonian function, we have formulated the optimality system for the nonlinear COVID-19 epidemic model. We have numerically solved the optimality system for the COVID-19 compartmental model using the efficient fourth-order Runge-Kutta iterative scheme with the forward-backward sweep method.

Keywords: optimal control; COVID-19; Pontryagin's maximum principle; forward-sweep method.

2010 AMS Subject Classification: 93E20.

*Corresponding author

E-mail address: nana.sacrifice@vvu.edu.gh

Received September 6, 2020

1. INTRODUCTION

The globally threatening respiratory illness; COVID-19, was identified first in Wuhan city, China in December, 2019. The Wuhan city became the epicenter of the deadly disease outbreak in China. The disease has since then spread across the globe, resulting in fear and panic in nations, causing the cancellation of major events in the world, such as postponement of sports seasons, compulsory closure of universities and colleges, and forcing many into self-imposed quarantine and isolation [1]. The disease invaded other countries and continents through the migration of infected people in China. The spreading of the disease to the different parts of the world caused Europe; especially, Italy, Spain, and France, to be the epicenters, and then the UK and the USA also became epicenters. Finally, the African continent, which was initially considered to be unfavorably continent for the disease, due to the hotness nature of its temperature, became susceptible to the disease [2]. The aggressiveness of the disease and its ability to cause fatalities in humans caused governments to impose partial and complete lockdowns [3].

According to (WHO 2020) [4], coronaviruses consist of viruses identified with causing illness, comprising of sicknesses such as the common cold and other complicated diseases. The virus is transmitted through contact with the droplets, sneezes, or exhales from the infected person or becoming contact with contaminated surfaces. Infected individuals may be symptomatic with headache, aches, cough, fever, dyspnea, sore throat, diarrhea, and loss of taste or smell. The COVID-19 infection can be prevented by adhering to the underlying measures: wearing of a face mask, application of hand sanitizers, regular washing of hand with soap under running water, avoidance of unnecessary mass gathering, social and personal distancing, self-isolation. As of September 3rd, 2020, COVID-19 global confirmed cases reported by WHO are $25,605,665$, with $852,758$ deaths, reported by WHO globally. The alarming number of intensified deaths and confirmed cases reported globally each day prompted the World Health Organization to declare the disease pandemic and consider it a global health emergency [5].

The study of infectious diseases using reliable mathematical and statistical modeling tools are very useful for understanding the spread of diseases in susceptible populations and can help

health policy makers to suggest possible control measures [6–14]. Even though it does not provide all-round insight to epidemic outbreaks, it has been of utmost importance to humans, as it employs scientific investigation to uncover the causes and effects of infection. The complex transmission dynamics of the 2019 coronavirus disease pandemic in the world has attracted a lot of attention in computational epidemiological modeling see, e.g., [15–31]. In [32], the authors generated a conceptual COVID-19 outbreak model in Wuhan considering the behavior reaction of the people and governmental actions. The estimates from the two main components of zoonotic introduction and emigration in 1918 influenza pandemic in London, United Kingdom were used to compute the disease's future trends, and the reporting ratio. In [33], Peng et al. proposed and discussed a model on the dynamics of COVID-19 in China. In [34], the authors examined the possibility of scrutinizing the available information on the ongoing outbreak of and evaluating the burden on healthcare systems by using an SIR model to project the actual numbers of infected cases, and identify Intensive care units and isolation wards burdens.

Sandar et al. [35], examined the COVID-19 transmission dynamics of a mathematical model which considered the difference in transmission between symptomatic and asymptomatic population and the lockdown effect on the disease. The effect of 21 days lockdown was assessed to lower the number of deaths and confirmed cases, using cases from three states in India. Hou et al. [36]; investigated the possibility of applying a three-stage SEIR meta-population model, which is in continuous-time, with consideration of the characteristics and the disease dynamics, to explain the spatial dynamics of the epidemic. In [37], a transmission network model of Bat-Host-Reservoir-People was formulated to determine the potentiality of the disease's transmission from infection source; bat to the host; human. Nishiura et al. [38] employed information from 28 infector-infectee pairs to derive the serial interval estimation of COVID-19. The estimation was done by collecting dates of infectors illnesses from the onset and that of infectee from research article and investigation reports, and analyses were performed on both. Zhang et al. [39] illustrated the possibility of MERS-CoV's transmissibility estimation and indicated the effective way of containing the infection from spreading by employing quantitative methodologies. Wu et al. [40], forecasted the national and global spread of COVID-19, by

effectively accounting for Wuhan's metropolitan-wide quarantine surrounding cities, from Jan $23-24,2020$. In [41], the authors examined the appropriate way of preventing COVID-19 at the various departmental levels of China by proposing a time series model that predicts the disease's trend. Based on the simulated results, various predictions were made about the future trend of the disease. In [42], a COVID-19 model was developed, which used stochastic transmission to evaluate the potency of contact tracing and isolation to curtail the disease.

In [43], the authors modified their existing transmission model of COVID-19 [44] by including contact and diagnosis rates that are time-dependent, to refit the available new data. With this, they predicted when the reproduction number would be less than 1. In [45], an application of spatial statistics, specifically, moran's I was employed to examine the spatial dynamics of the COVID-19 epidemic in mainland China. In [46], the authors examined the growth model of the three inflammatory lungs disease of MERS, SARS, and COVID-19, by considering the inhibition constant and growth rate of the diseases. The application of nonlinear fitting was used to determine the parameters of the models for the diseases. The results from the parametric analysis indicated that the COVID-19 growth rate is twice that of SARS and MERS. Sari et.al [47], introduced a simple SEIR model, which includes vaccination and treatment with the sole aim of minimizing the expose and infected. In [48], wang et al. estimated the trend of the COVID-19 epidemic in Wuhan with two assumptions of the basic reproduction number, by proposing a simple SEIR model for the disease dynamics.

The application of nonlinear differential equations with optimal control dynamics in epidemic modeling has widely been studied [49–77]. Djidjou-Demasse et al. [78] explored some useful control strategies that needs to be implemented to lower treatment costs and deaths of the infected individuals. Grigorieva et al. [79] described the COVID-19 spread in humans, using optimal control to derive an effective quarantine strategy for the SEIR model type. A COVID-19 optimal control mathematical that captures four time-dependent control functions is studied in [80]. In the work of the authors in [81], they developed and studied an epidemic deterministic

model for the transmission dynamics and control of COVID-19 disease. They constructed Lyapunov functions and investigated global stability for both disease-free and endemic equilibrium points. They also considered global sensitivity analysis and cost-effectiveness analysis in their study. Further recent works on optimal control modeling of COVID-19 infectious disease can be found in [82–87].

In this research article, a new compartmental SEIRW COVID-19 model is considered to describe the dynamics of the disease. Our present study is motivated by deterministic compartmental modeling concepts, nonlinear differential equations, optimal control theory, and the forward-backward sweep iterative method. This research is also inspired by the aforementioned literature on mathematical modeling of COVID-19 and other infectious diseases.

The rest of this research work is organized as follows: Section 2 deals with formulating a deterministic non-optimal control COVID-19 mathematical model. In section 3, local and global stability analysis are investigated. In section 4, a new SEIRW optimal control mathematical model is constructed and analyzed using personal protection, treatment, and spraying of disinfectant as time-dependent control functions. Finally, in section 5, optimal control strategies for the new Optimal control COVID-19 model are numerically solved and simulations results are discussed.

2. COVID-19 Mathematical Model

We construct a new compartmental SEIRW model to describe the dynamics of the disease. The population under consideration at time t is separated into susceptible $S(t)$, exposed $E(t)$, infected $I(t)$ and recovered $R(t)$. $W(t)$ present the virus in the environment. Let Λ_N denotes the recruitment rate of susceptible individuals. The model assumed that the susceptible get the disease through contact with an exposed individual at a rate β_1. The susceptible can again have the disease through contact with a contaminated environment at rate β_2. This assumption is contained in the research of [88], which confirmed people becoming infected when they come in contact with surfaces contaminated with the virus. This happens as a result of the exposed and infected individuals shedding the environment, especially through droplets, sneezes, or exhales.

Exposed individuals enter the infected class at a rate γ. Recovered individuals move to the recovery class at a rate λ. The exposed and infected individuals shed the environment at rates b and α, respectively. Let δ be the disease induced death in humans and η, decay rate of the virus in the environment. All individual classes leave the population through natural death μ. The dynamics for the model are presented in the schematic of Fig. 1.

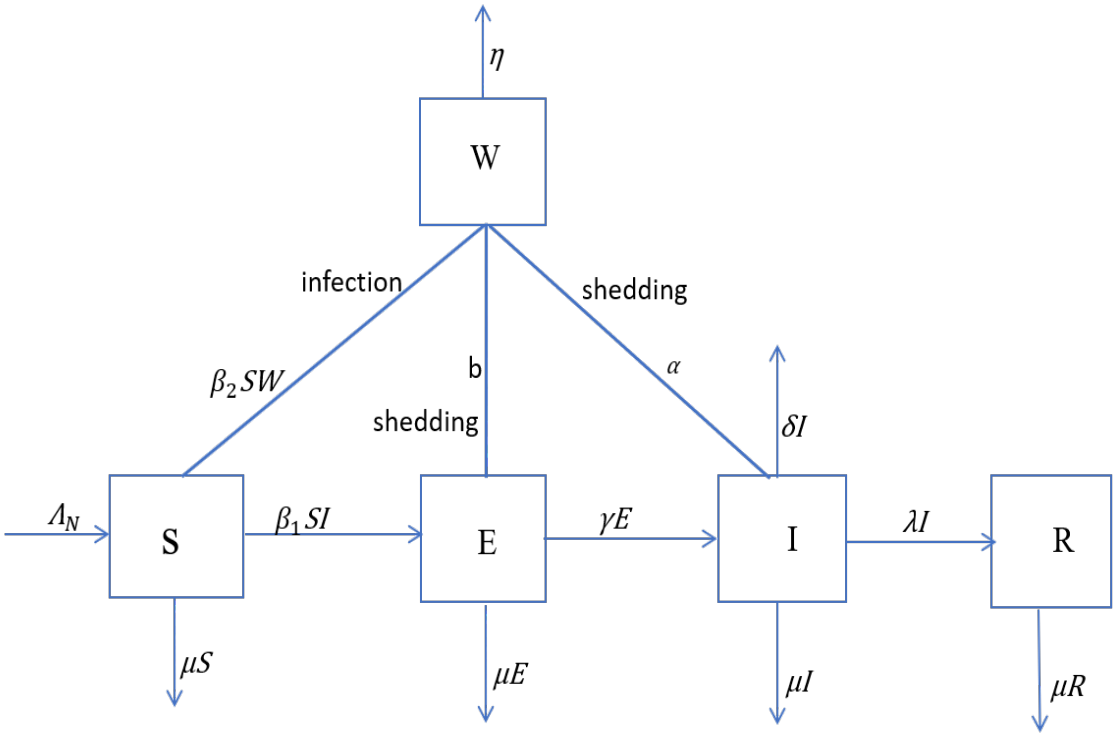

FIGURE 1. Flowchart of the model.

Based on these assumptions and the presentation in the flowchart, the differential equations describing the model are given as:

$$
(1)\qquad \begin{cases} \dfrac{dS}{dt} &= \Lambda_N - \beta_1 SI - \beta_2 SW - \mu S \\ \dfrac{dE}{dt} &= \beta_1 SI + \beta_2 SW - \gamma E - \mu E \\ \dfrac{dI}{dt} &= \gamma E - \delta I - \lambda I - \mu I \\ \dfrac{dR}{dt} &= \lambda I - \mu R \\ \dfrac{dW}{dt} &= bE + \alpha I - \eta W \end{cases}
$$

All involving parameters are nonnegative and defined in Table 1 below.

TABLE 1. **Parameters of the COVID-19 model**

Parameter	**Description**	**value**	**Reference**
η	Decay rate of COVID-19 virus in the environment	0.1	Assumed
α	Shedding rate of Symptomatic individuals	0.04	[19]
b	Shedding rate of Asymptomatic individuals	0.04	[19]
Λ_N	Recuitment rate of Susceptible individuals	$1.2 * 10^3$	Assumed
λ	Recovered rate of human individuals	0.0036	[37]
μ	Average lifespan of humans	0.0000391	Assumed
$\frac{1}{\gamma}$	Extrinsic incubation period of COVID-19 virus in humans	0.07143	[37]
δ	Disease induced death rate	0.1	[89]
β_1	Effective contact rate of Asymptomatic individuals	$(1.5-3)$	[90]
β_2	Effective contact rate of Susceptible individuals with the environment	$(1.5-3)$	[90]

2.1. Existence of disease-free equilibrium and the reproduction number. The COVID-19 model has a disease-free equilibrium (DFE), determined by equating the right-hand side of the equations in the model (1) to zero, given by:

$$E_0 = (S_0, E_0, I_0, R_0, W_0) = \Big(\frac{\Lambda_N}{\mu}, 0, 0, 0, 0\Big).$$

The basic reproduction number of the model at $E_0 = (S_0, E_0, I_0, R_0, W_0)$ is determined by employing the results of the next-generation matrix of Driessche et al. [91]. We deduced the following matrices based on [91],

$$F = \begin{bmatrix} 0 & \beta_1 S & \beta_2 S \\ 0 & 0 & 0 \\ 0 & 0 & 0 \end{bmatrix}, \quad V = \begin{bmatrix} (\gamma+\mu) & 0 & 0 \\ -\gamma & (\delta+\lambda+\mu) & 0 \\ -b & -\alpha & \eta \end{bmatrix}$$

Hence, the basic reproduction number for the COVID-19 model (1) is obtain by calculating the spectral radius of the matrix $\rho(FV^{-}1)$ as:

$$R_0 = \frac{\Lambda_N \gamma \beta_1}{\mu(\gamma+\mu)(\delta+\lambda+\mu)} + \frac{\Lambda_N \alpha \gamma \beta_2}{\mu\eta(\gamma+\mu)(\delta+\lambda+\mu)} + \frac{\Lambda_N \beta_2 b}{\mu\eta(\gamma+\mu)} \tag{2}$$

2.2. Existence of endemic equilibrium. Consider the model system (1); there exist a unique endemic equilibrium, denoted by;

$EQ = (S^*, E^*, I^*, R^*, W^*)$, with,

$$S^* = \frac{\Lambda_N}{R_0}$$

$$E^* = \frac{\eta(R_0-\mu)(\delta+\lambda+\mu)}{(\beta_1\eta\gamma+\beta_2 b(\delta+\lambda+\mu)+\beta_2\alpha\gamma)}$$

$$I^* = \frac{\gamma\eta(R_0-\mu)}{(\beta_1\eta\gamma+\beta_2 b(\delta+\lambda+\mu)+\beta_2\alpha\gamma)}$$

$$R^* = \frac{\lambda\gamma\eta(R_0-\mu)}{\mu(\beta_1\eta\gamma+\beta_2 b(\delta+\lambda+\mu)+\beta_2\alpha\gamma)}$$

$$W^* = \frac{(R_0-\mu)b(\delta+\lambda+\mu)+\alpha\gamma}{(\beta_1\eta\gamma+\beta_2 b(\delta+\lambda+\mu)+\beta_2\alpha\gamma)}$$

3. STABILITY-DISEASE FREE EQUILIBRIUM

Theorem 1. *When $R_0 < 1$, the disease-free equilibrium E_0 of the dynamical COVID-19 model (1) is asymptotically stable.*

Proof. By evaluating the Jacobian matrix at the disease-free equilibrium, we obtained the simplified Jacobian matrix given by

$$J_{E_0} = \begin{bmatrix} -\mu & 0 & \frac{-\beta_1\Lambda_N}{\mu} & 0 & \frac{-\beta_2\Lambda_N}{\mu} \\ 0 & -(\gamma+\mu) & \frac{\beta_1\Lambda_N}{\mu} & 0 & \frac{\beta_2\Lambda_N}{\mu} \\ 0 & \gamma & -(\delta+\lambda+\mu) & 0 & 0 \\ 0 & 0 & \lambda & -\mu & 0 \\ 0 & b & \alpha & 0 & -\eta \end{bmatrix}$$

clearly $P_1 = -\mu < 0$ and $P_2 = -\mu < 0$. The remaining matrix of J_{E_0} is;

$$A = \begin{bmatrix} -(\gamma+\mu) & \frac{\beta_1\Lambda_N}{\mu} & \frac{\beta_2\Lambda_N}{\mu} \\ \gamma & -(\delta+\lambda+\mu) & 0 \\ b & \alpha & -\eta \end{bmatrix}$$

The characteristic equation of the remaining matrix is given by;

$$P^3 + m_1P^2 + m_2P + m_3 = 0, \tag{3}$$

with, $a=-(\gamma+\mu)$, $b_1=\dfrac{\beta_1\Lambda_N}{\mu}$, $c=\dfrac{\beta_2\Lambda_N}{\mu}$, $d=\gamma$, $e=-(\delta+\lambda+\mu)$, $f=b$, $g=\alpha$, $h=-\eta$.

where

$m_1=-[a+e+h]$

$m_2=[ae+ah+eh-b_1d-cf]$

$m_3=[b_1dh+cfe-aeh-cdg]$

From the Routh-Hurwitz criterion [92], the characteristic equation will have negative real parts provided $m_1m_2>m_3>0$. Hence the disease-free equilibrium is locally asymptotically stable if and only if these conditions hold, otherwise unstable. □

Theorem 2. *The disease free equilibrium* $E_0=(S_0,E_0,I_0,R_0,W_0)=\left(\dfrac{\Lambda_N}{\mu},0,0,0,0\right)$ *is globally asymptotically stable in* R^5_+ *if* $R_0<1$.

Proof. We construct a Lyapunov function $L(S,E,I,R,W):R^5\to R^+$, for the steady state equilibrium point (disease free) defined as

$$L=\left(\frac{\gamma k_1\beta_1+\alpha\gamma\beta_2+bk_3\beta_2}{k_1k_2k_3}\right)E+\left(\frac{\gamma k_1\beta_1+\alpha\gamma\beta_2+bk_3\beta_2}{\gamma k_2k_3}\right)I+(S-S_0),$$

where $k_1=\eta$, $k_2=(\gamma+\mu)$ and $k_3=(\delta+\lambda+\mu)$.

Then the time derivative of L is given by;

$$\frac{dL}{dt}=\left(\frac{\gamma k_1\beta_1+\alpha\gamma\beta_2+bk_3\beta_2}{k_1k_2k_3}\right)\frac{dE}{dt}+\left(\frac{\gamma k_1\beta_1+\alpha\gamma\beta_2+bk_3\beta_2}{\gamma k_2k_3}\right)\frac{dI}{dt}+\frac{dS}{dt}$$

By substituting the right-hand sides of $\frac{dS}{dt}$, $\frac{dE}{dt}$ and $\frac{dI}{dt}$ into $\frac{dL}{dt}$, we obtain;

$$\frac{dL}{dt} = \left(\frac{\gamma k_1\beta_1 + \alpha\gamma\beta_2 + bk_3\beta_2}{k_1k_2k_3}\right)\Big(\beta_1 SI + \beta_2 SW - k_2E\Big) + \left(\frac{\gamma k_1\beta_1 + \alpha\gamma\beta_2 + bk_3\beta_2}{\gamma k_2k_3}\right)\Big(\gamma E - k_3 I\Big) + \Big(\Lambda_N - \beta_1 SI - \beta_2 SW - \mu S\Big)$$

$$\frac{dL}{dt} = \left(\frac{\gamma k_1\beta_1 + \alpha\gamma\beta_2 + bk_3\beta_2}{k_1k_2k_3}\right)\Big(\beta_1 SI + \beta_2 SW\Big) - \left(\frac{\gamma k_1\beta_1 + \alpha\gamma\beta_2 + bk_3\beta_2}{k_1k_3}\right)E + \left(\frac{\gamma k_1\beta_1 + \alpha\gamma\beta_2 + bk_3\beta_2}{k_1k_3}\right)E - \left(\frac{\gamma k_1\beta_1 + \alpha\gamma\beta_2 + bk_3\beta_2}{\gamma k_1k_3}\right)I + \Big(\Lambda_N - \beta_1 SI - \beta_2 SW - \mu S\Big)$$

$$\frac{dL}{dt} = \left(\frac{\gamma k_1\beta_1 + \alpha\gamma\beta_2 + bk_3\beta_2}{k_1k_2k_3}\right)\Big(\beta_1 SI + \beta_2 SW\Big) - \left(\frac{\gamma k_1\beta_1 + \alpha\gamma\beta_2 + bk_3\beta_2}{\gamma k_1}\right)I + \Big(\Lambda_N - \beta_1 SI - \beta_2 SW - \mu S\Big)$$

Since $(S_0 = \frac{\Lambda_N}{\mu})$ at the disease-free equilibrium,

$$\frac{dL}{dt} = \frac{\Lambda_N}{\mu}\left(\left(\frac{\gamma k_1\beta_1 + \alpha\gamma\beta_2 + bk_3\beta_2}{k_1k_2k_3}\right)\Big(\beta_1 I + \beta_2 W\Big) - \Big(\beta_1 I + \beta_2 W\Big)\right) - \left(\frac{\gamma k_1\beta_1 + \alpha\gamma\beta_2 + bk_3\beta_2}{\gamma k_1}\right)I$$

$$\frac{dL}{dt} = (R_0 - 1)\Big(\beta_1 I + \beta_2 W\Big) - \left(\frac{\gamma k_1\beta_1 + \alpha\gamma\beta_2 + bk_3\beta_2}{\gamma k_1}\right)I$$

It follows that $\frac{dL}{dt} \leq 0$ for $R_0 \leq 1$. Also it can clearly be seen that, $\frac{dL}{dt} = 0$ provided $I = 0$ and $W = 0$. Hence from [93], the disease-free equilibrium, E_0 is globally asymptotically stable when $R_0 < 1$. □

3.1. Stability-Endemic Equilibrium.

Theorem 3. *The endemic equilibrium $EQ = (S^*, E^*, I^*, R^*, W^*)$ for the COVID-19 model (1) is locally asymptotically stable when $R_0 > 1$.*

Proof. The Jacobian matrix J_{EQ} evaluated at the endemic equilibrium $(S^*, E^*, I^*, R^*, W^*)$ is given by

$$J_{EQ} = \begin{bmatrix} -\beta_1 I^* - \beta_2 W^* - \mu & 0 & -\beta_1 S^* & 0 & -\beta_2 S^* \\ \beta_1 I^* + \beta_2 W^* & -(\gamma+\mu) & \beta_1 S^* & 0 & \beta_2 S^* \\ 0 & \gamma & -(\delta+\lambda+\mu) & 0 & 0 \\ 0 & 0 & \lambda & -\mu & 0 \\ 0 & b & \alpha & 0 & -\eta \end{bmatrix}$$

let $C_{11} = -\beta_1 I^* - \beta_2 W^* - \mu$, $C_{13} = -\beta_1 S^*$, $C_{15} = -\beta_2 S^*$,

$C_{21} = \beta_1 I^* + \beta_2 W^*$, $C_{22} = -(\gamma+\mu)$, $C_{23} = \beta_1 S^*$, $C_{23} = \beta_2 S^*$,

$C_{32} = \gamma$, $C_{33} = -(\delta+\lambda+\mu)$,

$C_{43} = \lambda$, $C_{44} = -\mu$,

$C_{52} = b$, $C_{53} = \alpha$, $C_{55} = -\eta$.

The characteristic equation of J_{EQ} is given by

$$P^5 + D_1 P^4 + D_2 P^3 + D_3 P^2 + D_4 P + D_5 = 0. \tag{4}$$

where

$$D_1 = -(C_{11} + C_{22} + C_{33} + C_{44} + C_{55})$$

$$D_2 = (C_{11}C_{22} + C_{11}C_{33} + C_{11}C_{44} + C_{11}C_{55} + C_{22}C_{33} + C_{22}C_{44} + C_{22}C_{55} + C_{33}C_{44} + C_{33}C_{55} + C_{44}C_{55})$$

$$D_3 = (C_{11}C_{22}C_{33} + C_{11}C_{22}C_{44} + C_{11}C_{22}C_{55} + C_{11}C_{33}C_{44} + C_{11}C_{33}C_{55} + C_{11}C_{44}C_{55} + C_{22}C_{33}C_{44} + C_{22}C_{33}C_{55} + C_{22}C_{44}C_{55} + C_{33}C_{44}C_{55} + C_{13}C_{21}C_{32} + C_{21}C_{52} - C_{23}C_{32})$$

$$D_4 = (C_{11}C_{22}C_{33}C_{44} + C_{11}C_{22}C_{33}C_{55} + C_{11}C_{22}C_{44}C_{55} + C_{11}C_{33}C_{44}C_{55} + C_{22}C_{33}C_{44}C_{55} + C_{25}C_{32}C_{53} + C_{23}C_{32}C_{44} + C_{23}C_{32}C_{55} + C_{21}C_{33}C_{52} + C_{21}C_{44}C_{52} - C_{21}C_{32}C_{53} - C_{13}C_{21}C_{32}C_{44} - C_{13}C_{21}C_{32}C_{55} - C_{33}C_{52} - C_{44}C_{55})$$

$$D_5 = (C_{11}C_{22}C_{33}C_{44}C_{55} + C_{13}C_{21}C_{32}C_{44}C_{55} + C_{21}C_{32}C_{44}C_{53} + C_{33}C_{44}C_{52} - C_{23}C_{32}C_{44}C_{55} - C_{21}C_{33}C_{44}C_{52} - C_{25}C_{32}C_{53})$$

Routh Hurtwiz criterion [92], provides the conditions for determining the stability of (4), as; $D_1D_2D_3 > D_3^2 + D_1^2D_4$ and $(D_1D_4 - D_5)(D_1D_2D_3 - D_3^2 - D_1^2D_4) > D_5(D_1D_2 - D_3)^2 + D_1D_5^2$. If these condition are satisfied, the endemic equilibrium will be asymptotically stable, otherwise unstable. □

Theorem 4. *Given that $S = S^*$, $E = E^*$, $I = I^*$, $R = R^*$ and $W = W^*$, then, the endemic equilibrium of the mathematical model (1) is said to be globally asymptotically stable if $R_0 > 1$ and unstable if $R_0 < 1$.*

Proof. Let define a Lyapunov function, $L : \{(S,E,I,R,W) \in \tau_1 \mid S,E,I,R,W > 0\} \longrightarrow \mathbf{R}$ given by

$$L(S,E,I,R,W) = \left(S - S^* - S^* \ln\left(\frac{S}{S^*}\right)\right) + \left(E - E^* - E^* \ln\left(\frac{E}{E^*}\right)\right) + \left(I - I^* - I^* \ln\left(\frac{I}{I^*}\right)\right) + \left(R - R^* - R^* \ln\left(\frac{R}{R^*}\right)\right) + \left(W - W^* - W^* \ln\left(\frac{W}{W^*}\right)\right),$$

Differentiating L with respect to time.

$$\frac{dL}{dt} = \left(\frac{S - S^*}{S}\right)\frac{dS}{dt} + \left(\frac{E - E^*}{E}\right)\frac{dE}{dt} + \left(\frac{I - I^*}{I}\right)\frac{dI}{dt} + \left(\frac{R - R^*}{R}\right)\frac{dR}{dt} + \left(\frac{W - W^*}{W}\right)\frac{dW}{dt}$$

$$\frac{dL}{dt} = \left(\frac{S-S^*}{S}\right)\left(\Lambda_N - \beta_1 SI - \beta_2 SW - \mu S\right) + \left(\frac{E-E^*}{E}\right)\left(\beta_1 SI + \beta_2 SW - \gamma E - \mu E\right)$$
$$+\left(\frac{I-I^*}{I}\right)\left(\gamma E - \delta I - \lambda I - \mu I\right) + \left(\frac{R-R^*}{R}\right)\left(\lambda I - \mu R\right) + \left(\frac{W-W^*}{W}\right)\left(bE + \alpha I - \eta W\right)$$

$$\frac{dL}{dt} = \left(\frac{S-S^*}{S}\right)\left(\Lambda_N - \beta_1(S-S^*)(I-I^*) - \beta_2(S-S^*)(W-W^*) - \mu(S-S^*)\right)$$
$$+\left(\frac{E-E^*}{E}\right)\left(\beta_1(S-S^*)(I-I^*) + \beta_2(S-S^*)(W-W^*) - \gamma(E-E^*) - \mu(E-E^*)\right)$$
$$+\left(\frac{I-I^*}{I}\right)\left(\gamma(E-E^*) - \delta(I-I^*) - \lambda(I-I^*) - \mu(I-I^*)\right)$$
$$+\left(\frac{R-R^*}{R}\right)\left(\lambda(I-I^*) - \mu(R-R^*)\right) + \left(\frac{W-W^*}{W}\right)\left(b(E-E^*) + \alpha(I-I^*)\right.$$
$$\left.-\eta(W-W^*)\right)$$

$$\frac{dL}{dt} = \left(\Lambda_N\left(\frac{S-S^*}{S}\right) - \beta_1\left(\frac{(S-S^*)^2}{S}\right)(I-I^*) - \beta_2\left(\frac{(S-S^*)^2}{S}\right)(W-W^*) - \mu\left(\frac{(S-S^*)^2}{S}\right)\right)$$
$$+\left(\beta_1(S-S^*)\left(\frac{E-E^*}{E}\right)(I-I^*) + \beta_2(S-S^*)\left(\frac{(E-E^*)}{E}\right)(W-W^*) - \gamma\left(\frac{(E-E^*)^2}{E}\right)\right.$$
$$\left.-\mu\left(\frac{(E-E^*)^2}{E}\right)\right) + \left(\gamma(E-E^*)\left(\frac{(I-I^*)}{I}\right) - \delta\left(\frac{(I-I^*)^2}{I}\right)\right.$$
$$\left.-\lambda\left(\frac{(I-I^*)^2}{I}\right) - \mu\left(\frac{(I-I^*)^2}{I}\right)\right)$$
$$+\left(\lambda(I-I^*)\left(\frac{(R-R^*)}{R}\right) - \mu\left(\frac{(R-R^*)^2}{R}\right) + b(E-E^*)\left(\frac{(W-W^*)}{W}\right)\right.$$
$$\left.+\alpha(I-I^*)\left(\frac{W-W^*}{W}\right) - \eta\left(\frac{(W-W^*)^2}{W}\right)\right.$$

which gives;

$$\begin{aligned}\frac{dL}{dt} &= \Lambda_N - \Lambda_N\frac{S^*}{S} - \beta_1\left(\frac{(S-S^*)^2}{S}\right)(I-I^*) - \beta_2\left(\frac{(S-S^*)^2}{S}\right)(W-W^*) - \mu\left(\frac{(S-S^*)^2}{S}\right)\\ &+ \beta_1(S-S^*)(I-I^*) - \beta_1\frac{E^*}{E}(S-S^*)(I-I^*) + \beta_2(S-S^*)\left(\frac{(E-E^*)}{E}\right)(W-W^*)\\ &- \gamma\left(\frac{(E-E^*)^2}{E}\right) - \mu\left(\frac{(E-E^*)^2}{E}\right) + \gamma(E-E^*)\left(\frac{(I-I^*)}{I}\right)\\ &- \delta\left(\frac{(I-I^*)^2}{I}\right) - \lambda\left(\frac{(I-I^*)^2}{I}\right)\\ &- \mu\left(\frac{(I-I^*)^2}{I}\right) + \lambda(I-I^*)\left(\frac{(R-R^*)}{R}\right) - \mu\left(\frac{(R-R^*)^2}{R}\right)\\ &+ b(E-E^*) - b\frac{W^*}{W}(E-E^*) + \alpha(I-I^*) - \alpha(I-I^*) - \alpha\frac{W^*}{W}(I-I^*)\\ &- \eta\left(\frac{(W-W^*)^2}{W}\right).\end{aligned}$$

Grouping the above expression provides the equation;

$\frac{dL}{dt} = Q_1 - Q_2$, with,

$$\begin{aligned}Q_1 &= \Lambda_N + \beta_1(S-S^*)(I-I^*) + \beta_2(S-S^*)\left(\frac{(E-E^*)}{E}\right)(W-W^*) + \gamma(E-E^*)\left(\frac{(I-I^*)}{I}\right)\\ &+ \lambda(I-I^*)\left(\frac{(R-R^*)}{R}\right) + b(E-E^*) + \alpha(I-I^*)\end{aligned}$$

$$\begin{aligned}Q_2 &= \Lambda_N\frac{S^*}{S} + \beta_1\left(\frac{(S-S^*)^2}{S}\right)(I-I^*) + \beta_2\left(\frac{(S-S^*)^2}{S}\right)(W-W^*) + \mu\left(\frac{(S-S^*)^2}{S}\right)\\ &+ \beta_1\frac{E^*}{E}(S-S^*)(I-I^*) + \gamma\left(\frac{(E-E^*)^2}{E}\right) + \mu\left(\frac{(E-E^*)^2}{E}\right) + \delta\left(\frac{(I-I^*)^2}{I}\right)\\ &+ \lambda\left(\frac{(I-I^*)^2}{I}\right) + \alpha(I-I^*) + \mu\left(\frac{(I-I^*)^2}{I}\right) + \mu\left(\frac{(R-R^*)^2}{R}\right) + b\frac{W^*}{W}(E-E^*)\\ &+ \eta\left(\frac{(W-W^*)^2}{W}\right).\end{aligned}$$

Clearly, the inequality $Q_1 < Q_2$ can be confirmed, indicating $\frac{dL}{dt} \leq 0$ when $Q_1 < Q_2$. Hence, it can be verified that $\frac{dL}{dt} = 0$, when $S = S^*$, $E = E^*$, $I = I^*$, $R = R^*$ and $W = W^*$. This implies that the largest compact invariant set $\{(S,E,I,R,W) \in \tau_1 : \frac{dL}{dt} = 0\}$ is the singleton $\{EQ\}$, where EQ is the endemic equilibrium. Hence, from [93], EQ is globally asymptotically stable in τ_1. □

4. Optimal Control COVID-19 SEIRW Model

In this section, we develop and analyze a new optimal control COVID-19 SEIRW dynamic model. We consider three multiple time-dependent control functions for our optimal control model formulation consisting of ν_1, denoting personal protection, ν_2, denoting treatment of the infected individuals and ν_3, denoting spraying of the environment with disinfectant. For the personal protection time-dependent control, we can think of wearing of face mask, application of hand sanitizer, regular washing of hand with soap under running water, social distancing, self-isolation, and other important preventive measures. The main aim for constructing this new SEIRW optimal problem is to minimise the number of exposed and infected individuals in the human population. For this purpose, we seek to minimise the objective functional given by;

$$J(\nu_1,\nu_2,\nu_3) = \int_0^{t_f} \left[h_1 E + h_2 I + \frac{1}{2}(n_1\nu_1^2 + n_2\nu_2^2 + n_3\nu_3^2)\right] dt \tag{5}$$

subject to

$$\begin{cases} \frac{dS}{dt} &= \Lambda_N - (1-\nu_1)(\beta_1 SI + \beta_2 SW) - \mu S \\ \frac{dE}{dt} &= (1-\nu_1)(\beta_1 SI + \beta_2 SW) - \gamma E - \mu E \\ \frac{dI}{dt} &= \gamma E - (\delta + \lambda + \mu + r_0\nu_2) I \\ \frac{dR}{dt} &= \lambda I + r_0\nu_2 I - \mu R \\ \frac{dW}{dt} &= bE + \alpha I - \eta W - \tau\nu_3 W, \end{cases} \tag{6}$$

with control set defined as;

(7) $\mathscr{U} := \{\nu = (\nu_1, \nu_2, \nu_3) | \nu_j(t) \text{ is Lebesgue measurable}, 0 \leq \nu_i(t) \leq 1, t \in [0, t_f] \quad \text{for} \quad j = 1, 2, 3.\}$

The weight constants h_1 and h_2 are associated with exposed and infectious individuals respectively. Also the positive weights $n_1,\ n_2$ and n_3 are associated with time-dependent control functions $\nu_1,\ \nu_2$ and ν_3 respectively.

From equations (5) and (6), the Hamiltonian function related to the optimal control problem is given by

$$
\begin{aligned}
\mathbf{H} &= h_1 E + h_2 I + \frac{1}{2}(n_1 \nu_1^2 + n_2 \nu_2^2 + n_3 \nu_3^2) \\
&+ \vartheta_1 \Big[\Lambda_N - (1-\nu_1)(\beta_1 SI + \beta_2 SW) - \mu S\Big] \\
&+ \vartheta_2 \Big[(1-\nu_1)(\beta_1 SI + \beta_2 SW) - \gamma E - \mu E\Big] \\
&+ \vartheta_3 \Big[\gamma E - (\delta + \lambda + \mu + r_0 \nu_2) I\Big] \\
&+ \vartheta_4 \Big[\lambda I + r_0 \nu_2 I - \mu R\Big] \\
&+ \vartheta_5 \Big[bE + \alpha I - \eta W - \tau \nu_3 W\Big],
\end{aligned} \tag{8}
$$

We can determine an optimal solution for a given optimal control problem using the Pontryagin maximum principle developed and studied in [94]. Now, suppose that (ζ, ξ) represent an optimal control solution for a given dynamical optimal control problem, then there exist adjoint or co-state variables, $\varsigma = (\varsigma_1,\ \varsigma_2,\ \cdots, \varsigma_n)$ which satisfies the equation below

$$
\begin{cases}
\frac{d\zeta}{dt} = \frac{\partial \mathbf{H}(t,\ \zeta,\ \xi,\ \varsigma)}{\partial \varsigma}, \\
0 = \frac{\partial \mathbf{H}(t,\ \zeta,\ \xi,\ \varsigma)}{\partial \xi}, \\
\frac{d\varsigma}{dt} = -\frac{\partial \mathbf{H}(t,\ \zeta,\ \xi,\ \varsigma)}{\partial \zeta}.
\end{cases} \tag{9}
$$

By applying equation (9) and the Hamiltonian function (8), the adjoint state model or system and the optimal control characterisation for the optimal control problem are given in the theorem below.

Theorem 5. *Suppose that* $(\nu_1{}^*,\ \nu_2{}^*, \nu_3{}^*)$ *is an optimal control and suppose that* $(S^*, E^*, I^*, R^*, W^*)$ *is an optimal control solution for the dynamical optimal control problem (5)-(6) that minimize* $J(\nu_1, \nu_2, \nu_3)$ *over* $\mathscr{U}$*, then there exist adjoint variables* $\vartheta_1, \vartheta_2, \vartheta_3, \vartheta_4$ *and* ϑ_5 *that satisfies the dynamical model below.*

$$
\begin{aligned}
\frac{d\vartheta_1}{dt} &= (\vartheta_1 - \vartheta_2)(1-\nu_1)\beta_1 I + (\vartheta_1 - \vartheta_2)(1-\nu_1)\beta_2 W + \mu\vartheta_1 \\
\frac{d\vartheta_2}{dt} &= -h_1 + (\vartheta_2 - \vartheta_3)\gamma + \mu\vartheta_2 - b\vartheta_5 \\
\frac{d\vartheta_3}{dt} &= -h_2 + (\vartheta_1 - \vartheta_2)(1-\nu_1)\beta_1 S + (\vartheta_3 - \vartheta_4)\lambda + (\vartheta_3 - \vartheta_4)r_0\nu_2 + \delta\vartheta_3 - \alpha\vartheta_5 + \mu\vartheta_3 \\
\frac{d\vartheta_4}{dt} &= \mu\vartheta_4 \\
\frac{d\vartheta_5}{dt} &= (\vartheta_1 - \vartheta_2)(1-\nu_1)\beta_2 S + \eta\vartheta_5
\end{aligned}
$$

with transversality conditions

$$\vartheta_j(T) = 0, \quad j \in \{1,2,3,4,5\}. \tag{10}$$

with control functions $(\nu_1^*,\ \nu_2^*,\ \nu_3^*)$ *which satisfies the optimality condition given by*

$$
\begin{cases}
\nu_1^* &= min\left\{1, max\left\{0, \left((\vartheta_2 - \vartheta_1)\dfrac{\beta_1 SI}{n_1} + (\vartheta_2 - \vartheta_1)\dfrac{\beta_2 SW}{n_1}\right)\right\}\right\} \\
\nu_2^* &= min\left\{1, max\left\{0, (\vartheta_3 - \vartheta_4)\dfrac{r_0 I}{n_2}\right\}\right\} \\
\nu_3^* &= min\left\{1, max\left\{0, (\vartheta_5)\dfrac{\tau W}{n_3}\right\}\right\}
\end{cases} \tag{11}
$$

Proof. In order to obtain the co-state dynamical model and the transversality conditions, we need to apply the well-known Maximum Principle constructed and studied in [94] to partially differentiate the Hamiltonian function (8) as follows:

$$\begin{cases} \dfrac{d\vartheta_1}{dt} = -\dfrac{\partial \mathbf{H}}{\partial S}, \\ \dfrac{d\vartheta_2}{dt} = -\dfrac{\partial \mathbf{H}}{\partial E}, \\ \dfrac{d\vartheta_3}{dt} = -\dfrac{\partial \mathbf{H}}{\partial I} \\ \dfrac{d\vartheta_4}{dt} = -\dfrac{\partial \mathbf{H}}{\partial R}, \\ \dfrac{d\vartheta_5}{dt} = -\dfrac{\partial \mathbf{H}}{\partial W}. \end{cases} \tag{12}$$

with

$$\vartheta_j(t_f) = 0, \quad j \in \{1,2,3,4,5\}. \tag{13}$$

Finally, to obtain the control characterization (11), we need to solve for u_1^*, u_2^* and u_3^* from the equation below.

$$\begin{cases} \dfrac{\partial \mathbf{H}}{\partial v_1} = 0, \\ \dfrac{\partial \mathbf{H}}{\partial v_2} = 0, \\ \dfrac{\partial \mathbf{H}}{\partial v_3} = 0. \end{cases} \tag{14}$$

□

5. Numerical Simulation and Discussion

This section deals with numerical simulations and results discussions for our optimality system. Since analytical solutions of nonlinear optimal control problems or systems is a very difficult task, we have therefore for this purpose used the fourth-order Runge-Kutta iterative scheme in MATLAB to generate our numerical solutions. We consider the following initial conditions: $S_0 = 880,\ E_0 = 100,\ I_0 = 40,\ R_0 = 10$ and $W_0 = 5$. The positive constants in the objective functional are assigned the following values: $h_1 = 10,\ h_2 = 10,\ n_1 = 10,\ n_2 = 5$ and $n_3 = 8$. The model parameter values for the various numerical simulation illustrations are provided in table 1.

5.1. Minimizing through controls v_1 and v_2. To contain the disease, the controls v_1 and v_2 are utilized to improve the objective functional to optimality. The exposed and infected plots showed the effectiveness of the strategy considered. Thus, with the controls v_1 and v_2, the exposed and infected plots of figure 2 showed a differentiable reduction in the graphs of control compared to the scenarios without control. This implies that the strategy of v_1 and v_2 is efficient in containing the disease from spreading.

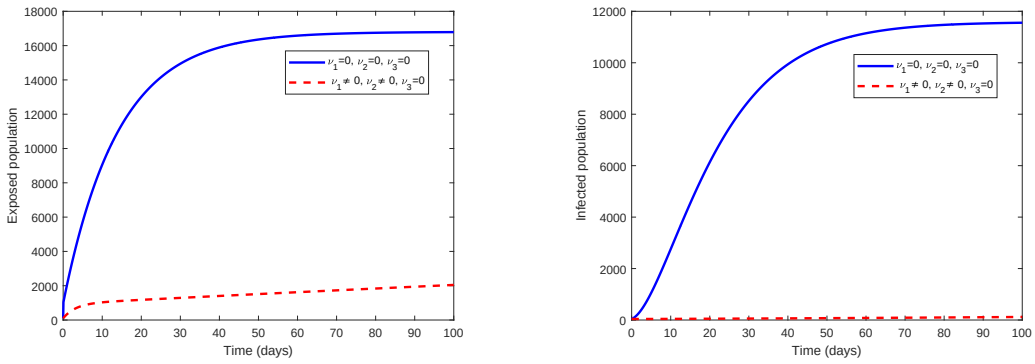

(a) (b)

FIGURE 2. Numerical solutions for the Exposed and Infected populations with $(v_1 \neq 0, v_2 \neq 0)$ and without optimal control functions

5.2. Minimizing through controls v_1 and v_3. The controls v_1 and v_3 are utilized to improve the objective functional to optimality. The exposed and infected plots showed the effectiveness of the strategy considered by displaying an observable difference in the plots of figure3. With the controls v_1 and v_3, the exposed and infected plots of figure 3 showed a drastic reduction in the control graphs compared to the graphs without control. This shows that the strategy of v_1 and v_3 is efficient in containing the disease from spreading.

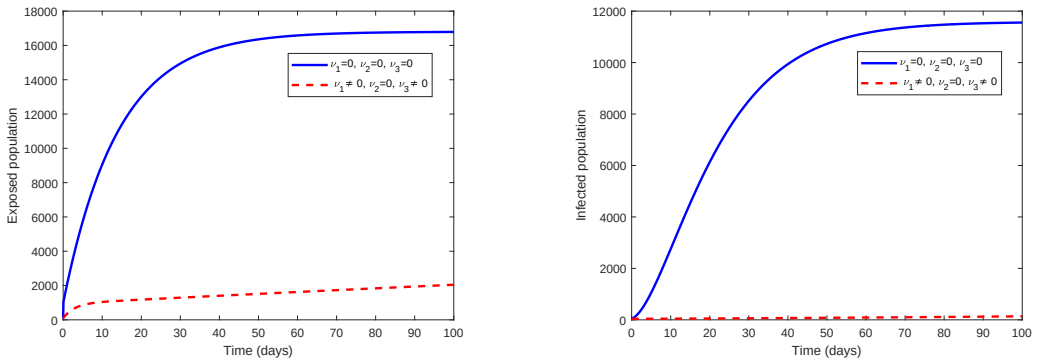

(a) (b)

FIGURE 3. Numerical solutions for the Exposed and Infected populations with $(v_1 \neq 0, v_3 \neq 0)$ and without optimal control functions

5.3. Minimizing through controls v_2 and v_3. To improve the objective functional to optimality, the controls v_2 and v_3 are utilized. The plots of the exposed and infected individuals as indicated in figure 4 showed an observable distinction in the control and without control graphs. The controls v_2 and v_3, provided the desired results of explicitly lowering the number of exposed and infected individuals, suggesting the effectiveness of this strategy.

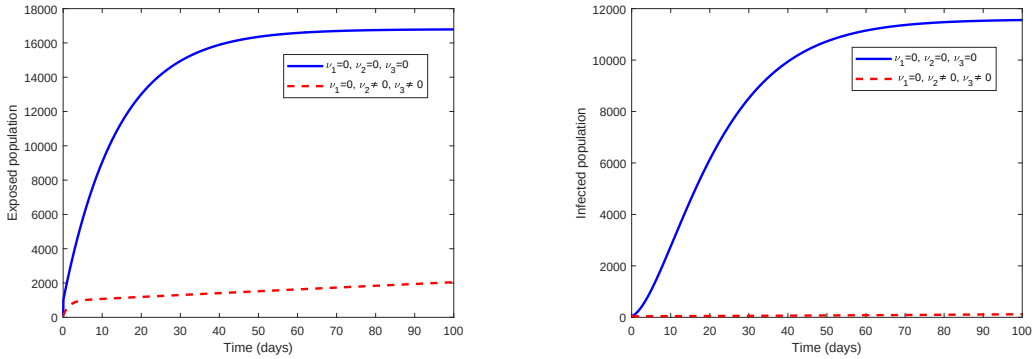

(a) (b)

FIGURE 4. Numerical solutions for the Exposed and Infected populations with $(\nu_2 \neq 0, \nu_3 \neq 0)$ and without optimal control functions

5.4. Minimizing through controls ν_1, ν_2 and ν_3. Finally, all the three controls are utilized to improve the objective functional to optimality. The exposed and infected plots of figure 5 showed the effectiveness of the strategy considered. The controls ν_1, ν_2 and ν_3, provided the desired results of explicitly minimizing the number of exposed and infected individuals. This is confirmed in the plots of figure 5 with the control graphs compared to the scenarios without control. This is an indication that the controls; ν_1, ν_2, and ν_3 are effective in containing the disease from spreading.

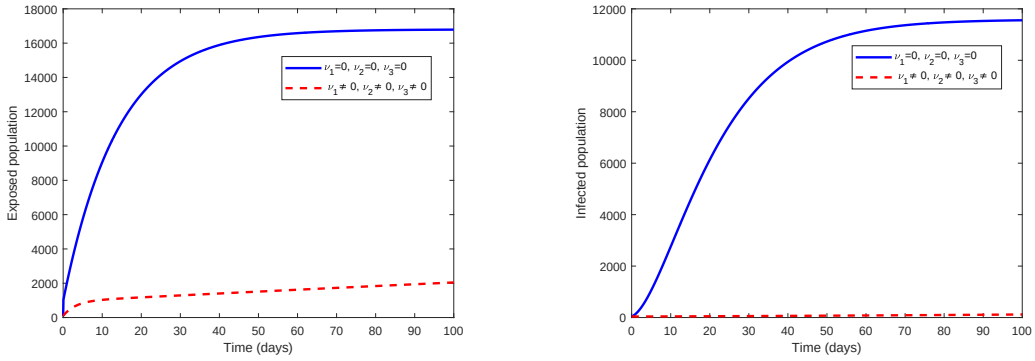

(a) (b)

FIGURE 5. Numerical solutions for the Exposed and Infected populations with $(\nu_1 \neq 0, \nu_2 \neq 0, \nu_3 \neq 0)$ and without optimal control functions

5.5. Control profiles. Finally, figure 6 represents the optimal control plot of personal protection, spraying the environment with disinfectant and treatment of infected individuals.

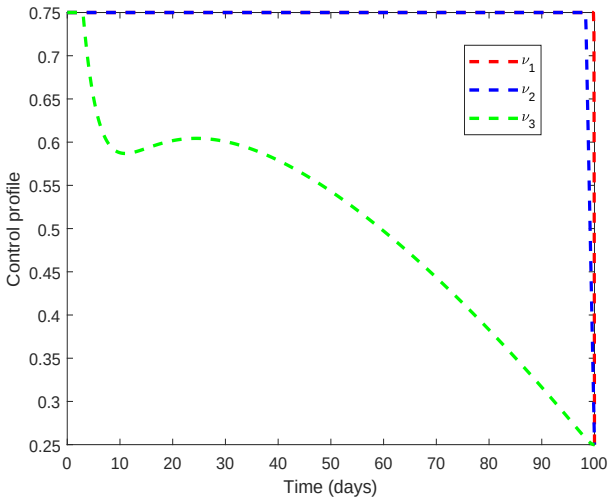

FIGURE 6. control profile.

5.6. Conclusion. In this article, a new compartmental SEIRW COVID-19 model is introduced and analyzed. We derived the model equilibria (disease-free and endemic) and the basic reproduction number for the non-optimal control SEIRW epidemic model. Stability analysis for the nonlinear SEIRW COVID-19 model is locally and globally investigated. In this study, we have used mathematical modeling concepts in optimal control theory to explore some control strategies by formulating a new optimal control problem that describes the dynamics of the deadly COVID-19 disease. The control model was analyzed by utilizing the Pontryagin's maximum principle, to derive the optimality system for the SEIRW COVID-19 model. We have generated some interesting numerical results using fourth-order Runge-Kutta scheme with the forward-backward sweep method, which is one of the most reliable and efficient iterative schemes for nonlinear dynamical optimal control problems. The simulated results proved the incomparable impact of the control strategies considered by substantially reducing the exposed and infected individuals in the population.

DATA AVAILABILITY

Our mathematical modeling does not include data. All parameter values that were used for our simulations have been cited accordingly.

CONFLICT OF INTERESTS

The authors declare that there is no conflict of interest.

REFERENCES

[1] D.B. Jernigan, CDC COVID-19 Response Team, Update: Public Health Response to the Coronavirus Disease 2019 Outbreak — United States, February 24, 2020, MMWR Morb. Mortal. Wkly. Rep. 69 (2020), 216–219.

[2] CDC COVID-19 Response Team. Severe outcomes among patients with coronavirus disease 2019 (COVID-19) - United States, February 12–March 16, 2020. MMWR Morb Mortal Wkly Rep. 69(2020), 343–346.

[3] J.F. Myers, R.E. Snyder, C.C. Porse, et al. Identification and Monitoring of International Travelers During the Initial Phase of an Outbreak of COVID-19 — California, February 3–March 17, 2020, MMWR Morb. Mortal. Wkly. Rep. 69 (2020), 599–602.

[4] World Health Organization. Global surveillance for COVID-19 caused by human infection with COVID-19 virus: interim guidance, 20 march 2020. World Health Organization. (2020).

[5] WHO coronavirus disease (COVID-19) dashboard. World Health Organization website. Updated July 30, 2020. https://covid19.who.int/. 2020

[6] J. Panovska-Griffiths, Can mathematical modelling solve the current Covid-19 crisis? BMC Public Health. 20 (2020), 551.

[7] N. Ferguson, D. Laydon, G. Nedjati Gilani, et al. Report 9: Impact of non-pharmaceutical interventions (NPIs) to reduce COVID19 mortality and healthcare demand, Imperial College London, 2020. https://doi.org/10.25561/77482.

[8] N.G. Davies, A.J. Kucharski, R.M. Eggo, et al. Effects of non-pharmaceutical interventions on COVID-19 cases, deaths, and demand for hospital services in the UK: a modelling study, Lancet Public Health. 5 (2020), e375–e385.

[9] R.M. Anderson, R.M. May. Infectious diseases of humans: dynamics and control. Oxford, Oxford University Press, New York, 1991.

[10] R.N. Thompson, Epidemiological models are important tools for guiding COVID-19 interventions, BMC Med. 18 (2020), 152.

[11] G. Chowell, C. Castillo-Chavez, P.W. Fenimore, C.M. Kribs-Zaleta, L. Arriola, J.M. Hyman, Model Parameters and Outbreak Control for SARS, Emerg. Infect. Dis. 10 (2004), 1258–1263.

[12] M. Kretzschmar, J. Wallinga, Mathematical Models in Infectious Disease Epidemiology, in: A. Krämer, M. Kretzschmar, K. Krickeberg (Eds.), Modern Infectious Disease Epidemiology, Springer New York, New York, NY, 2009: pp. 209–221.

[13] H.W. Hethcote, The Mathematics of Infectious Diseases, SIAM Rev. 42 (2000), 599–653.

[14] S.A. Levin, New Directions in the Mathematics of Infectious Disease, in: C. Castillo-Chavez, S. Blower, P. van den Driessche, D. Kirschner, A.-A. Yakubu (Eds.), Mathematical Approaches for Emerging and Reemerging Infectious Diseases: Models, Methods, and Theory, Springer New York, New York, NY, 2002: pp. 1–5.

[15] L. Lopez, X. Roda. A Modified SEIR model to predict COVID-19 outbreak in Spain and Italy: simulating control scenarios and multi scale epidemics. Preprint at https://www.medrxiv.org/content/10.1101/2020.03.27.20045005v3. (2020).

[16] M.A. Acuna-Zegarra, A. Comas-Garcia, E. Hernandez-Vargas, et al. The SARS-CoV-2 epidemic outbreak: a review of plausible scenarios of containment and mitigation for Mexico, Epidemiology, Preprint at https://www.medrxiv.org/content/10.1101/2020.03.28.20046276v1. (2020).

[17] D. Chowell, G. Chowell, K. Roosa, R. Dhillon, D. Srikrishna, Sustainable social distancing through face-mask use and testing during the Covid-19 pandemic, Infectious Diseases (except HIV/AIDS), Preprint at https://www.medrxiv.org/content/10.1101/2020.04.01.20049981v3. (2020).

[18] N.H Shah, A.H Suthar, E.N Jayswal. Control strategies to curtail transmission of covid-19. Int. J. Math. Math. Sci. 2020 (2020), 2649514.

[19] S.M. Kassa, J.B.H. Njagarah, Y.A. Terefe, Analysis of the mitigation strategies for COVID-19: From mathematical modelling perspective, Chaos Solitons Fractals. 138 (2020), 109968.

[20] C.N. Ngonghala, E. Iboi, S. Eikenberry, M. Scotch, C.R. MacIntyre, M.H. Bonds, A.B. Gumel, Mathematical assessment of the impact of non-pharmaceutical interventions on curtailing the 2019 novel Coronavirus, Math. Biosci. 325 (2020), 108364.

[21] Z. Yang, Z. Zeng, K. Wang, et al. Modified SEIR and AI prediction of the epidemics trend of COVID-19 in China under public health interventions, J. Thorac. Dis. 12 (2020), 165–174.

[22] L. Hébert-Dufresne, B.M. Althouse, S.V. Scarpino, A. Allard, Beyond R_0: Heterogeneity in secondary infections and probabilistic epidemic forecasting, ArXiv:2002.04004 [Physics, q-Bio]. (2020).

[23] M. Batista, Estimation of the final size of the coronavirus epidemic by SIR model, Research Gate, 2020.

[24] Z. Bai, Y. Gong, X. Tian, Y. Cao, W. Liu, J. Li, The Rapid Assessment and Early Warning Models for COVID-19, Virol. Sin. 35 (2020), 272–279.

[25] A. Senapati, S. Rana, T. Das, J. Chattopadhyay, Impact of intervention on the spread of COVID-19 in India: A model based study, ArXiv:2004.04950 [Math, q-Bio]. (2020).

[26] P. Boldog, T. Tekeli, Z. Vizi, A. Dénes, F.A. Bartha, G. Röst, Risk Assessment of Novel Coronavirus COVID-19 Outbreaks Outside China, J. Clin. Med. 9 (2020), 571.

[27] Y. Fang, Y. Nie, M. Penny, Transmission dynamics of the COVID-19 outbreak and effectiveness of government interventions: A data-driven analysis, J. Med. Virol. 92 (2020), 645–659.

[28] F. Petropoulos, S. Makridakis. Forecasting the novel coronavirus COVID-19. PLoS ONE. 15(3) (2020), e0231236.

[29] X.M. Rong, L. Yang, H.D. Chu, M. Fan, Effect of delay in diagnosis on transmission of COVID-19. Math. Biosci. Eng. 17(3) (2020), 2725–2740.

[30] S. He, S. Tang, L. Rong, A discrete stochastic model of the covid-19 outbreak: Forecast and control, Math. Biosci. Eng. 17 (2020), 2792–2804.

[31] Q. Li, X. Guan, P. Wu, et al. Early Transmission Dynamics in Wuhan, China, of Novel Coronavirus–Infected Pneumonia, N. Engl. J. Med. 382 (2020), 1199–1207.

[32] Q. Lin, S. Zhao, D. Gao, et al. A conceptual model for the coronavirus disease 2019 (COVID-19) outbreak in Wuhan, China with individual reaction and governmental action, Int. J. Infect. Dis. 93 (2020), 211–216.

[33] L. Peng, W. Yang, D. Zhang, C. Zhuge, L. Hong, Epidemic analysis of COVID-19 in China by dynamical modeling, ArXiv:2002.06563 [q-Bio]. (2020).

[34] W.-K. Ming, J. Huang, C.J.P. Zhang, Breaking down of healthcare system: Mathematical modelling for controlling the novel coronavirus (2019-ncov) outbreak in wuhan, china. Preprint at https://www.biorxiv.org/CONTENT/10.1101/2020.01.27.922443V2. (2020).

[35] T. Sardar, S.S. Nadim, S. Rana, J. Chattopadhyay, Assessment of Lockdown Effect in Some States and Overall India: A Predictive Mathematical Study on COVID-19 Outbreak, Chaos Solitons Fractals. 139 (2020), 110078.

[36] J. Hou, J. Hong, B. Ji, et al. Changing transmission dynamics of covid-19 in china: a nationwide population-based piecewise mathematical modelling study. Preprint at https://www.medrxiv.org/content/10.1101/2020.03.27.20045757v1. (2020).

[37] T.-M. Chen, J. Rui, Q.-P. Wang, Z.-Y. Zhao, J.-A. Cui, L. Yin, A mathematical model for simulating the phase-based transmissibility of a novel coronavirus, Infect. Dis. Poverty. 9 (2020), 24.

[38] H. Nishiura, N.M. Linton, A.R. Akhmetzhanov, Serial interval of novel coronavirus (COVID-19) infections, Int. J. Infect. Dis. 93 (2020), 284–286.

[39] X.-S. Zhang, R. Pebody, A. Charlett, et al. Estimating and modelling the transmissibility of Middle East Respiratory Syndrome CoronaVirus during the 2015 outbreak in the Republic of Korea, Influenza Other Respir. Viruses. 11 (2017), 434–444.

[40] J.T. Wu, K. Leung, G.M. Leung, Nowcasting and forecasting the potential domestic and international spread of the 2019-nCoV outbreak originating in Wuhan, China: a modelling study, Lancet. 395 (2020), 689–697.

[41] J. Cao, X. Jiang, B. Zhao, et al. Mathematical modeling and epidemic prediction of covid-19 and its significance to epidemic prevention and control measures. J. Biomed. Res. Innov. 1(1) (2020), 1–19.

[42] J. Hellewell, S. Abbott, A. Gimma, et al. Feasibility of controlling COVID-19 outbreaks by isolation of cases and contacts, Lancet Glob. Health. 8 (2020), e488–e496.

[43] B. Tang, N.L. Bragazzi, Q. Li,et al. An updated estimation of the risk of transmission of the novel coronavirus (2019-ncov). Infect. Dis. Model. 5 (2020), 248–255.

[44] B. Tang, X. Wang, Q. Li, et al. Estimation of the transmission risk of the 2019-ncov and its implication for public health interventions. J. Clinic. Med. 9(2) (2020), 462.

[45] D. Kang, H. Choi, J.-H. Kim, J. Choi, Spatial epidemic dynamics of the COVID-19 outbreak in China, Int. J. Infect. Dis. 94 (2020), 96–102.

[46] K. Liang, Mathematical model of infection kinetics and its analysis for COVID-19, SARS and MERS, Infect. Genet. Evol. 82 (2020), 104306.

[47] R.A. Sari, U. Habibah, A. Widodo. Optimal control on model of sars disease spread with vaccination and treatment. J. Exp. Life Sci. 7(2) (2017), 61–68.

[48] H. Wang, Z. Wang, Y. Dong, et al. Phase-adjusted estimation of the number of Coronavirus Disease 2019 cases in Wuhan, China, Cell Discov. 6 (2020), 10.

[49] J.K. Asamoah, F.T. Oduro, E. Bonyah, B. Seidu, Modelling of rabies transmission dynamics using optimal control analysis. J. Appl. Math. 2017 (2017), 2451237.

[50] E. Bonyah, K. Badu, S.K. Asiedu-Addo, Optimal control application to an Ebola model, Asian Pac. J. Trop. Biomed. 6 (2016), 283–289.

[51] E. Bonyah, M.A. Khan, K.O. Okosun, J.F. Gómez-Aguilar. On the co-infection of dengue fever and zika virus. Opt. Control Appl. Meth. 40(3) (2019), 394–421.

[52] M. Ghosh, S. Olaniyi, O.S. Obabiyi. Mathematical analysis of reinfection and relapse in malaria dynamics. Appl. Math. Comput. 373 (2020), 125044.

[53] J.O. Akanni, S. Olaniyi, F.O. Akinpelu, Global asymptotic dynamics of a nonlinear illicit drug use system, J. Appl. Math. Comput. https://doi.org/10.1007/s12190-020-01423-7. (2020).

[54] S. Nana-Kyere, J. Ackora-Prah, E. Okyere, S. Marmah, T. Afram. Hepatitis b optimal control model with vertical transmission. Appl. Math. 7(1) (2017), 5–13.

[55] Y. Chitour, F. Jean, P. Mason. Optimal control models of goal-oriented human locomotion. SIAM J. Control Optim. 50(1) (2012), 147–170.

[56] L. Chen, J. Sun. Global stability and optimal control of an sirs epidemic model on heterogeneous networks. Physica A., Stat. Mech. Appl. 410 (2014), 196–204.

[57] K. Wickwire. Mathematical models for the control of pests and infectious diseases: a survey. Theor. Popul. Biol. 11(2) (1977), 182–238.

[58] H.R. Joshi. Optimal control of an hiv immunology model. Opt. Control Appl. Meth. 23(4) (2002), 199–213.

[59] M. Salathé, J. Jones. Dynamics and control of diseases in networks with community structure. PLoS Comput. Biol. 6(4) (2010), e1000736.

[60] A. Korobeinikov, E. Khailov, E. Grigorieva, Optimal control for an epidemic in populations of varying size, in: Dynamical Systems and Differential Equations, Proceedings of the 10th AIMS International Conference (Madrid, Spain), American Institute of Mathematical Sciences, 2015: pp. 549–561.

[61] D. Kirschner, S. Lenhart, S. Serbin. Optimal control of the chemotherapy of HIV. J. Math. Biol. 35(7) (1997), 775–792.

[62] M.H.A. Biswas, L.T. Paiva, MdR de Pinho. A seir model for control of infectious diseases with constraints. Math. Biosci. Eng. 11(4) (2014), 761.

[63] B.R.E. Rowthorn, F. Toxvaerd. The optimal control of infectious diseases via prevention and treatment. CEPR Discussion Paper No. DP8925, https://ssrn.com/abstract=2034143. (2012).

[64] H. Behncke. Optimal control of deterministic epidemics. Opt. Control Appl. Meth. 21(6) (2000), 269–285.

[65] T.K. Kar, A. Batabyal. Stability analysis and optimal control of an sir epidemic model with vaccination. Biosystems, 104(2-3) (2011), 127–135.

[66] K.O. Okosun, O. Rachid, N. Marcus. Optimal control strategies and cost-effectiveness analysis of a malaria model. BioSystems. 111(2) (2013), 83–101.

[67] Z. Feng, Y. Yang, D. Xu, et al. Timely identification of optimal control strategies for emerging infectious diseases. J. Theor. Biol. 259 (2009), 165–171.

[68] Y. Ding, Z. Wang, H. Ye. Optimal control of a fractional-order hiv-immune system with memory. IEEE Trans. Control Syst. Technol. 20(3) (2011), 763–769.

[69] C. Castilho. Optimal control of an epidemic through educational campaigns. Electron. J. Differ. Equ. 2006(2006), 125.

[70] M.D. Ahmad, M. Usman, A. Khan, M. Imran. Optimal control analysis of ebola disease with control strategies of quarantine and vaccination. Infect. Dis. Poverty, 5(1) (2016), 72.

[71] G. Zaman, Y.H. Kang, I.H. Jung. Stability analysis and optimal vaccination of an sir epidemic model. BioSystems, 93(3) (2008), 240–249.

[72] A.D. Liddo. Optimal control and treatment of infectious diseases. the case of huge treatment costs. Mathematics, 4(2) (2016), 21.

[73] R.L.M. Neilan, E. Schaefer, H. Gaff, et al. Modeling optimal intervention strategies for cholera. Bull. Math. Biol. 72(8) (2010), 2004–2018.

[74] J.J. Kutch, P. Gurfil, Optimal control of HIV infection with a continuously-mutating viral population, in: Proceedings of the 2002 American Control Conference (IEEE Cat. No.CH37301), IEEE, Anchorage, AK, USA, 2002: pp. 4033–4038 vol.5.

[75] Elsa KS Hansen. Applications of optimal control theory to infectious disease modeling. PhD thesis, (2011).

[76] S. Nana-Kyere, R.H. Doe, F.A. Boateng, et al. Optimal control model of malaria disease with standard incidence rate. J. Adv. Math. Computer Sci. 23(5) (2017) JAMCS.35011.

[77] M. Imran, T. Malik, A.R. Ansari, A. Khan. Mathematical analysis of swine influenza epidemic model with optimal control. Japan J. Ind. Appl. Math. 33 (2016), 269–296.

[78] R. Djidjou-Demasse, Y. Michalakis, M. Choisy, M.T. Sofonea, S. Alizon, Optimal COVID-19 epidemic control until vaccine deployment, Infectious Diseases (except HIV/AIDS), Preprint at https://www.medrxiv.org/content/10.1101/2020.04.02.20049189v3. (2020).

[79] E. Grigorieva, E. Khailov, A. Korobeinikov, Optimal quarantine strategies for COVID-19 control models, ArXiv:2004.10614 [Math]. (2020).

[80] S.E. Moore, E. Okyere, Controlling the Transmission Dynamics of COVID-19, ArXiv:2004.00443 [Math, q-Bio]. (2020).

[81] J. Asamoah, M. Owusu, Z. Jin, et al. Global stability and cost-effectiveness analysis of covid-19 considering the impact of the environment: using data from Ghana. Chaos Solitons Fractals. 140 (2020), 110103.

[82] D.B. Jernigan, CDC COVID-19 Response Team, Update: Public Health Response to the Coronavirus Disease 2019 Outbreak — United States, February 24, 2020, MMWR Morb. Mortal. Wkly. Rep. 69 (2020), 216–219.

[83] S.İ. Araz, Analysis of a Covid-19 model: Optimal control, stability and simulations, Alexandria Engineering Journal. In Press. https://doi.org/10.1016/j.aej.2020.09.058.

[84] D. Aldila, M. Z. Ndii, B. M. Samiadji, Optimal control on COVID-19 eradication program in Indonesia under the effect of community awareness, Math. Biosci. Eng. 17 (2020) 6355–6389.

[85] L.L. Obsu, S.F. Balcha. Optimal control strategies for the transmission risk of covid-19. J. Biol. Dyn. 14(2020), 590–607.

[86] A. Perkins, G. Espana, Optimal control of the COVID-19 pandemic with non-pharmaceutical interventions, Preprint at https://www.medrxiv.org/content/10.1101/2020.04.22.20076018v1. (2020).

[87] N.R. Sasmita, M. Ikhwan, S. Suyanto, V. Chongsuvivatwong, Optimal control on a mathematical model to pattern the progression of coronavirus disease 2019 (COVID-19) in Indonesia, Glob. Health Res. Policy. 5 (2020), 38.

[88] J.A. Otter, C. Donskey, S. Yezli, et al. Transmission of sars and mers coronaviruses and influenza virus in healthcare settings: the possible role of dry surface contamination. J. Hosp. Infect. 92(3) (2016), 235–250.

[89] S.E. Eikenberry, M. Mancuso, E. Iboi, et al. To mask or not to mask: Modeling the potential for face mask use by the general public to curtail the COVID-19 pandemic, Infect. Dis. Model. 5 (2020), 293–308.

[90] N.G. Becker, K. Glass, B. Barnes, et al. Using mathematical models to assess responses to an outbreak of an emerged viral respiratory disease. Final Report to the Australian Government Department of Health and Ageing. National Centre for Epidemiology and Population Health, Australian National University, (2006).

[91] P. van den Driessche, J. Watmough, Reproduction numbers and sub-threshold endemic equilibria for compartmental models of disease transmission, Math. Biosci. 180 (2002), 29–48.

[92] R.N. Clark. The routh-hurwitz stability criterion, revisited. IEEE Control Syst. Mag. 12(3) (1992), 119–120.

[93] J.P La Salle. The stability of dynamical systems. SIAM, 1976.

[94] L.S. Pontryagin, V.G. Boltyanskii, R.V. Gamkrelidze, E.F. Mishchenko. The mathematical theory of optimal processes. Wiley, New York, NY, 1962.